

Lensless Ultra-Miniature Imagers Using Odd-Symmetry Spiral Phase Gratings

Patrick R. Gill and David G. Stork

Rambus Labs, 1050 Enterprise Way, Suite 700, Sunnyvale, California, 94089, USA
pgill@rambus.com

Abstract: We introduce a new type of diffractive element based on odd-symmetry phase gratings. Spiral arrangements of these gratings over photosensors constitute a new class of unprecedentedly-small computational camera.

© 2013 Optical Society of America

OCIS codes: 050.1970, 110.1758.

1. Introduction

We present a new type of diffractive imager smaller than cameras reliant on lenses and ray-optical focusing, yet with superior performance to diffractive imagers based on Talbot-effect angle-sensitive pixels (ASPs). [1–4] The smallest natural-illumination single-shot imagers exploit diffraction (but see [5] for a multi-shot approach). One traditional limitation of diffractive optics is that they contain structures specifically designed to function with monochromatic light, and thus their optical characteristics are typically wavelength-sensitive and of limited use under broad-spectrum illumination. Although diffractive ASP arrays can be used to make ultra-small, lensless imagers [2–4], such imagers suffer from technical and fundamental obstacles to high-resolution imaging [4, 6]. Here we introduce a new type of diffractive optic that enables an ultra-miniature, diffraction-based imager that overcomes the limitations of ASP-based imagers.

2. Odd-symmetry gratings

Our key insight is that it is possible to build diffractive structures which produce near-field, λ - and depth-robust null planes we call optical “curtains”. Curtains are a direct consequence of a certain type of odd symmetry in the profile of a phase grating. The existence of curtains enhances a lensless imager’s robustness by ensuring that the location of nulls on a photosensor can be predicted geometrically, and are not excessively λ - or depth-sensitive.

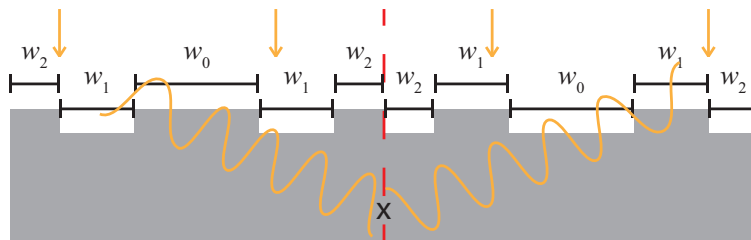


Fig. 1. Geometry of phase grating ensuring odd spatial symmetry and destructive interference at point x for normally-incident light. Thicker regions of the phase grating introduce a phase delay of π relative to thinner regions. The specific arrangement of length segments w_0 , w_1 and w_2 guarantee compliance with Eq. 2. For every contribution to the electric field at x caused by light incident through the grating at some distance to the left of x , there exists a contribution of the same magnitude but opposite phase caused by light incident to the same distance to the right of x . Thus x and all points on the red vertical line comprise a curtain.

A phase grating formed by a high- n , low-dispersion substrate and a low- n , high-dispersion coating can introduce approximately λ -independent phase shifts in all normally-incident visible light. If there exist certain points p on this

interface that satisfy the following symmetry in their transmission $t(\cdot)$ and phase retardation $\phi(\cdot)$,

$$t(p+y) = t(p-y) \quad \forall y \quad (1)$$

$$\phi(p+y) = \phi(p-y) + \pi + 2n\pi \quad \forall y, n \in \mathbb{I}, \quad (2)$$

where y is a horizontal translation transverse to the grating direction, then the grating has odd symmetry about points p , and light will interfere destructively below p , regardless of λ and depth z . The geometry guaranteeing this destructive interference is illustrated in Fig. 1. We omit the proof here, but it is possible to show that every phase grating with λ - and depth-robust curtains must also have the symmetry properties of Eqs. 1 and 2. Curtains persist when incident angle is perturbed; their locations shift laterally by an amount proportional to incident angle. Odd symmetry has been used to shape Fraunhofer diffraction in Dammann gratings [7], but to our knowledge this is its first application to imaging using near-field diffraction.

Figure 1 exhibits a binary phase grating with three free parameters w_0 , w_1 and w_2 , but in general binary odd-symmetry phase gratings can be made with any number of independently-chosen segments' lengths. The relatively few free parameters in a binary odd-symmetry phase grating facilitates computational searches for specific $\{w_0, w_1, \dots\}$ combinations yielding desirable properties. For example, a useful property of a $25\mu\text{m}$ -tall phase grating intended to image incoming light would be that visible light from a point source is maximally concentrated $25\mu\text{m}$ below the grating. Figure 2 shows scalar finite-difference time-domain (FDTD) wave simulations of the interaction of light with just such an optimized device with two different widths w_0 and w_1 .

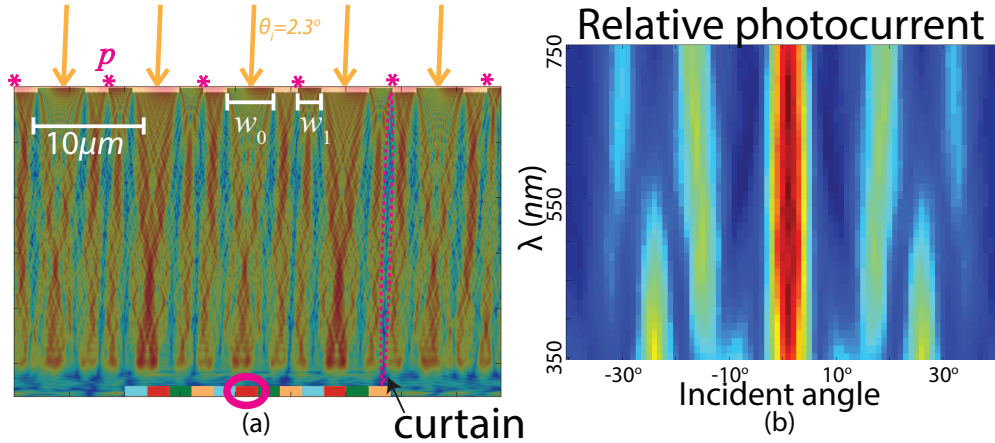


Fig. 2. Simulations of energy density showing operation of odd-symmetry phase gratings. (a) FDTD simulation of light incident at 2.3° interacting with an odd-symmetry phase grating. Red regions have higher electric field strength. Points p are indicated with asterisks. Multicolored boxes at the bottom of the device represent $2\mu\text{m}$ photodiodes, one of which is highlighted. (b) Simulated photocurrent of the photodiode highlighted in (a) for various incident angles and wavelengths. Note the relative consistency of the response over all visible wavelengths.

3. Imaging with odd-symmetry gratings

A linear odd-symmetry grating above a photosensor array could pass information from a single spatial orientation of features in the far field (that transverse to the grating orientation). However, to capture information about arbitrarily-oriented features of a complex scene, it is necessary to have a complete distribution of orientations in the diffractive optic. More generally, if the point-source responses (PSRs) are approximately spatially-invariant, the transfer function of the imager approximates convolution with the PSR function. In such a case, the PSR should have significant power at all 2D spatial frequencies to make the inversion problem of image recovery well-conditioned. Figure 3a shows a spatially-compact spiral ensemble of bending odd-symmetry gratings with no gaps in the 2D Fourier transform of its PSR (Fig. 3b). This design consists of six odd-symmetry gratings with one to four segments per odd-symmetry point.

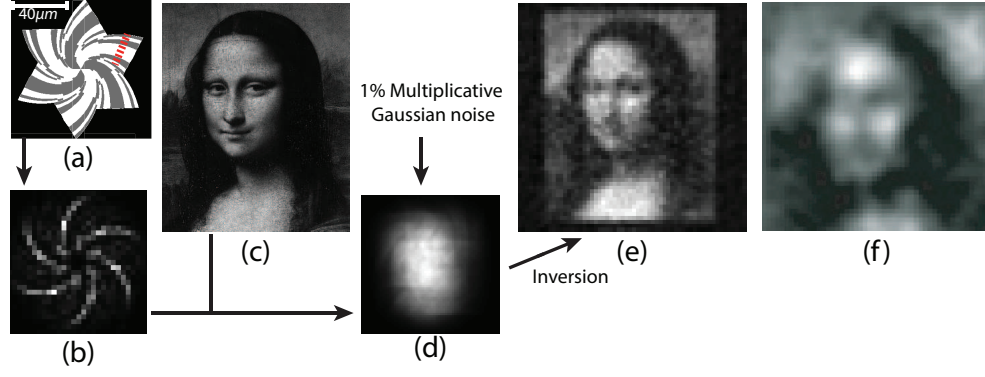


Fig. 3. Simulated imaging using a spiral ensemble of odd-symmetry phase gratings. (a) Spiral arrangement of odd-symmetry diffraction gratings. White and gray correspond to thick and thin phase grating segments, while black represents opaque regions. The cross section of the grating at the red dotted line is similar to a linear odd-symmetry grating. (b) Point-source response (PSR), derived from optical simulation, assuming a grating-pixel array separation of $100\text{ }\mu\text{m}$ and a $2.2\text{ }\mu\text{m}$ pixel pitch. (c) Ground truth input image. (d) Optical simulation of the photocurrent observed at a 60×60 sensor array with a $2.2\text{ }\mu\text{m}$ pixel pitch, including 1% multiplicative noise. (e) Reconstructed image using Tikhonov regularization. (f) Reconstruction of same test image using the device from [2], whose sensor area is a factor of 37 larger than ours.

Each grating is numerically optimized to focus visible light onto a photodetector array $100\text{ }\mu\text{m}$ below. To estimate the imaging performance of such a device, we optically simulated signals from a 60×60 pixel array with $2.2\text{ }\mu\text{m}$ pitch $100\text{ }\mu\text{m}$ below the gratings with the sensor illuminated by a complex scene (Fig. 3c) far ($\gg 100\text{ }\mu\text{m}$) from the sensor. While the photocurrent from the pixel array is itself unintelligible (Fig. 3d), using Tikhonov regularization, it is possible to reconstruct the scene (Fig. 3e) to a higher resolution than possible using a much larger ASP-based device (Fig. 3f) [2]. Compressed sensing techniques [8] could be applied to improve the reconstruction quality if the scene is known to have a compressible structure. Compressed sensing would be especially advantageous if small gaps in the Fourier transform of the PSR exist.

In conclusion, we have introduced a new class of optical imager based on a novel type of odd-symmetric phase grating coupled with an imaging array. The simulated performance of our $132\text{ }\mu\text{m} \times 132\text{ }\mu\text{m} \times 100\text{ }\mu\text{m}$ imager is qualitatively superior to the measured performance of the ASP-based lensless imager prototype whose volume is a factor of 3 larger and whose area is a factor of 37 larger. [2] Therefore, odd-symmetry-based imagers may be even better suited than ASP arrays to space-constrained imaging applications.

References

1. A. Wang, P. Gill, and A. Molnar, "Light field image sensors based on the Talbot effect," *Applied Optics* **48**, 5897–5905 (2009).
2. P. R. Gill, C. Lee, D.-G. Lee, A. Wang, and A. Molnar, "A microscale camera using direct Fourier-domain scene capture," *Optics Letters* **36**, 2949–2951 (2011).
3. P. R. Gill, C. Lee, S. Sivaramakrishnan, and A. Molnar, "Robustness of planar Fourier capture arrays to colour changes and lost pixels," *Journal of Instrumentation* **7**, C01,061 (2012).
4. P. Gill and A. C. Molnar, "Scaling properties of well-tiled PFCAs," in "Imaging Systems and Applications," (Optical Society of America, 2012).
5. M. F. Duarte, M. A. Davenport, D. Takhar, J. N. Laska, T. Sun, K. F. Kelly, and R. G. Baraniuk, "Single-pixel imaging via compressive sampling," *IEEE Signal Processing Magazine* **25**, 83–91 (2008).
6. A. Wang and A. Molnar, "A light-field image sensor in 180 nm CMOS," *IEEE Journal of Solid-State Circuits* **47**, 257–271 (2012).
7. R. L. Morrison, "Symmetries that simplify the design of spot array phase gratings," *JOSA A* **9**, 464–471 (1992).
8. D. L. Donoho, "Compressed sensing," *IEEE Transactions on Information Theory* **52**, 1289–1306 (2006).